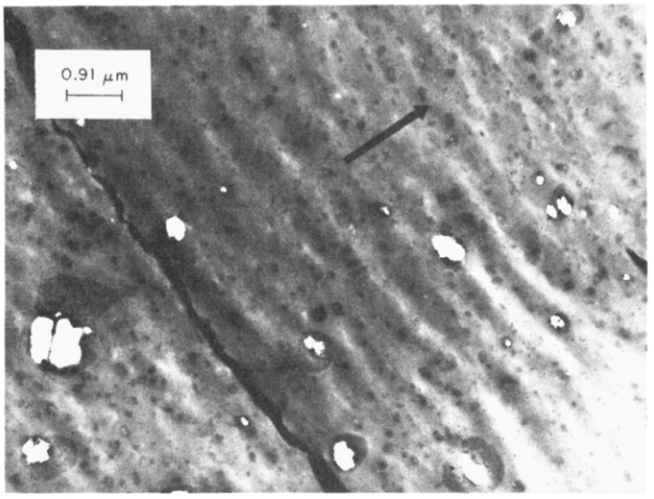

Figure 3. Cross-sectional micrograph of a pressed film of similar composition as Figure 1. The rheology, however, has been adjusted to produce abnormal spherical carboxylate domains (arrow). The dark line from upper left-hand corner to central bottom is due to foldover of the microtomed sample film.

Table I
Morphological Dependence of CE for 25% Carboxylate/75% Sulfonate Blends of Perfluorinated Ionomers

morphology	pred CE	obsd CE
spherical	62%	56%
lamellar	86%	89%

diction, this film has an abnormally low CE as shown in Table I.

In summary, we have extended the effective medium theory to track the morphological dependence of transport and dielectric properties of polymer composites. The utility of the theory is demonstrated with a successful delineation of ion selectivity in physical blends of two incompatible perfluorinated ionomers. Ways to improve and generalize this theory are discussed.

References and Notes

(1) Hobbs, S. Y. in "Plastics Polymer Science and Technology"; Baijal, M. D., Ed.; Wiley-Interscience: New York, 1982; pp 274–279.
(2) Hsu, W. Y.; Giri, M. R.; Ikeda, R. M. *Macromolecules* **1982**, *15*, 1210 and references therein.
(3) Straley, J. P. *Phys. Rev. B* **1977**, *15*, 5733. Cohen, M. H.; Jortner, J.; Webman, I. *Phys. Rev. B* **1978**, *17*, 4555 and references therein.
(4) Wood, D. M.; Ashcroft, N. W. *Philos. Mag.* **1977**, *35*, 269. Cohen, M. H.; Jortner, J. *Phys. Rev. Lett.* **1973**, *30*, 696 and references therein.
(5) Oriented spheroids are assumed to simplify the presentation and mathematics. The full conductivity and depolarization tensors are needed for ellipsoids of random orientations. Spheroids used in this model are either prolate ($a \geq b = c$) or oblate ($a = b \geq c$), where a, b, and c, are semiprincipal axes of an ellipsoid. The axis of revolution for the spheroid is along the semimajor axis a for the prolate case and along the semiminor axis c for the oblate case.
(6) The eccentricity e of a spheroid is $[1 - (c/a)^2]^{1/2}$, where $0 \leq c/a \leq 1$ is the aspect ratio. When e increases from 0 to 1, the spheroid morphology changes continuously from spherical to fibrillar in the prolate case and from spherical to lamellar in the oblate case.
(7) For transport and dielectric considerations, the appropriate susceptibilities are the conductivity $\sigma(\omega)$ and dielectric function $\epsilon(\omega)$, respectively. Each could be complex, but usually either the real or the imaginary component dominates, except under resonance.
(8) Stratton, J. A. "Electromagnetic Theory"; McGraw-Hill: New York, 1941; pp 207–217. Note that, for the geometry under consideration, the inside field E_i is always parallel to the far field (or the mean field) E.
(9) See, for example: Funke, K. In "Superionic Conductors"; Mahan, G. D., Roth, W. L., Eds.; Plenum Press: New York, 1976; p 185. The cited relation is in rationalized MKS units; to convert into Gaussian units, replace ϵ_0 by $(4\pi)^{-1}$.
(10) More exactly, the scaling[11] and analytic[12] theories predict $\sigma \propto (f - f_0)^t$ above the threshold and $\epsilon \propto |f - f_0|^{-s}$, where s and t are critical exponents that depend on the effective spatial dimensionality. For a comprehensive discussion of critical exponents, see: Nelson, D. R. *Nature (London)* **1979**, *269*, 379.
(11) Efros, A. L.; Shklovskii, B. I. *Phys. Status Solidi B* **1976**, *76*, 475.
(12) Bergman, D. J.; Imry, Y. *Phys. Rev. Lett.* **1977**, *39*, 1222.
(13) Hori, M.; Yonezawa, F. *J. Math. Phys.* **1975**, *16*, 352. Contributions from pairs, triplets, quadruplets, etc. are systematically added by this scheme.
(14) Granquist, C. G.; Hunderi, O. *Phys. Rev. B* **1978**, *18*, 1554. This phenomenological method results in replacing the quadratic eq 4 by a higher order algebraic equation; for spherical particles, it is in much better accord with numerical results[3] than simple effective medium theory.[4]
(15) Davidson, A.; Tinkham, M. *Phys. Rev. B* **1976**, *13*, 3261.
(16) The general chemical formulas for the perfluorinated ionomers are $[(CF_2)_nCFOR_fSO_3^-]_x$ and $[(CF_2)_nCFOR_fCO_2^-]_x$, respectively. The equivalent weight of the ionomers is about 1100.

William Y. Hsu*
Central Research and Development Department
E. I. du Pont de Nemours and Company
Experimental Station
Wilmington, Delaware 19898

Timothy D. Gierke
Polymer Products Department
E. I. du Pont de Nemours and Company
Washington Works, B21
Parkersburg, West Virginia 26101

Charles J. Molnar
Finishes and Fabricated Products Department
E. I. du Pont de Nemours and Company
Tralee Park Plant
Wilmington, Delaware 19898

Received August 22, 1983

Implications of the Failure of the Stokes–Einstein Equation for Measurements with QELSS of Polymer Adsorption by Small Particles

We have reported[1,2] that the Stokes–Einstein equation

$$D = k_B T / 6\pi\eta r \quad (1)$$

can fail noticeably for spherical probe particles in polymer–solvent solutions, even though the probe particles are very dilute. Here, D is the diffusion coefficient, $k_B T$ is the thermal energy, η is the solution viscosity, and r is the apparent hydrodynamic radius. This failure, which is not related to the failure of eq 1 in the case of interacting particles, was not altogether unexpected. Equation 1 is based on a continuum description of the solvent (i.e., solvent molecules much smaller than probe particles), but a probe particle in a polymer solution encounters molecules of its own size.

Measurements of D have been used to observe the occurrence of polymer binding by spherical particles.[3] Conversely, polymer binding to microscopic probe particles obscures experimental tests on D in polymer solutions.[4] We here discuss how adsorption isotherms may be obtained in a system in which eq 1 fails.

Quasi-elastic light scattering spectroscopy (QELSS) was used to find the diffusion coefficient of carboxylate-modified polystyrene latex spheres (Polysciences, Inc.) of radii

0024-9297/83/2216-1947$01.50/0

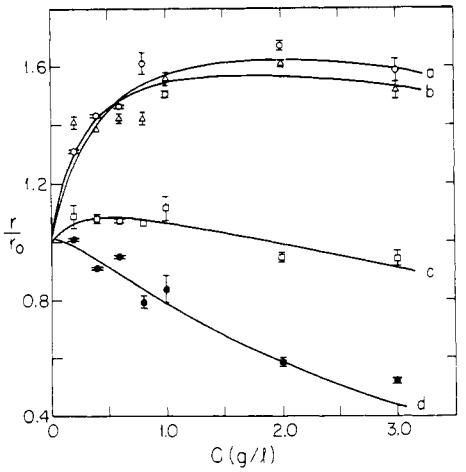

Figure 1. Dependence of the apparent hydrodynamic radii of (a) 208-Å, (b) 517-Å, (c) 0.322-μm, and (d) 0.655-μm spheres on the polymer concentration. Here, r_0 is r for a sphere in pure water.

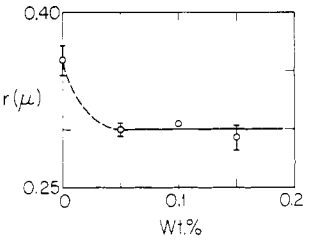

Figure 2. Effect of Triton X-100 on r of 0.322-μm spheres in 1.0 g/L polymer solution. Note that r for solutions containing Triton X-100 and no polymer is larger than r for solutions containing neither polymer nor Triton X-100.

208 Å, 517 Å, 0.322 μm, and 0.655 μm in poly(ethylene oxide) (Polysciences, Inc., MW = 300 000)–water solutions. Sphere concentrations were less than 5×10^{-2} wt %. The polymer was a commercial preparation and was not subjected to further fractionation. The polymer is not soluble in water at concentrations much greater than 3 g/L. Experimental methods were as described in ref 1; light scattered through 90° from a 25-mW, 6328-Å laser beam was observed. Data were analyzed by the method of cumulants; the signal-to-noise ratio was typically 500.

In Figure 1, the apparent hydrodynamic radius r (as normalized by the radius r_0 of the probe in pure water) is plotted against the polymer concentration c. The initial rise in r/r_0 may be attributed to polymer adsorption onto the probe surface.[3] However, as c and r_0 are increased, the apparent hydrodynamic radius falls. This cannot be attributed simply to polymer desorption, since the hydrodynamic radii of the larger spheres at higher polymer concentrations are less than those of the same spheres in pure water.

The physical effects responsible for the increases and for the decreases in r are seen more clearly if they are separated from each other. To prevent polymer binding, 0.1 wt % of the nonionic detergent Triton X-100 (poly(ethylene glycol *p*-isooctylphenyl ether)) (Sigma) was added to each system.[5] In the absence of polymer, the radii of the smaller spheres are 15–20 Å larger in water–Triton X-100 than in pure water, the increased radius presumably being adsorbed detergent. Figure 2 shows the apparent hydrodynamic radius of the 0.322-μm spheres in 1.0 g/L polymer solution as a function of Triton concentration. The radius is independent of the Triton concentration c_T, at least for $c_T > 0$, indicating that there is no competition between polymer and detergent binding. The apparent hydrodynamic radius r_T of the Triton-coated spheres is reduced by the added polymer, the mechanism of the reduction being the polymer-induced failure of the Stokes–Einstein equation, as shown in Figure 3.

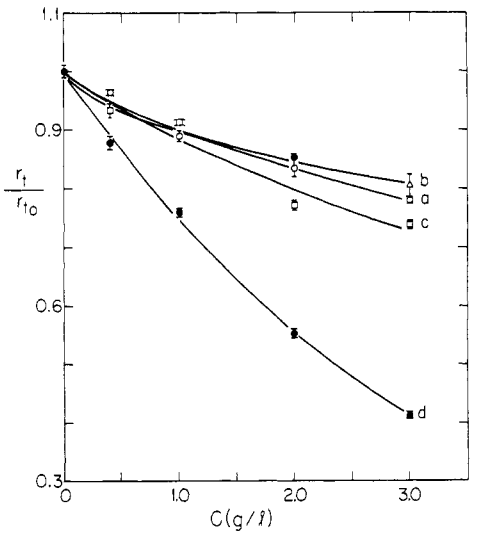

Figure 3. Apparent radii of spheres in water–poly(ethylene oxide)–0.1 wt % Triton X-100 as a function of polymer concentration, showing the failure of the Stokes–Einstein equation when the probe and the other dissolved molecules are comparable in size. The smooth curves represent fits of the data to eq 2 with (208-Å spheres) $k_1 = 0.11$, $k_2 = 0.78$; (517-Å spheres) $k_1 = 0.11$, $k_2 = 0.61$; (0.322-μm spheres) $k_1 = 0.12$, $k_2 = 0.861$; and (0.655-μm spheres) $k_1 = 0.29$, $k_2 = 1.01$.

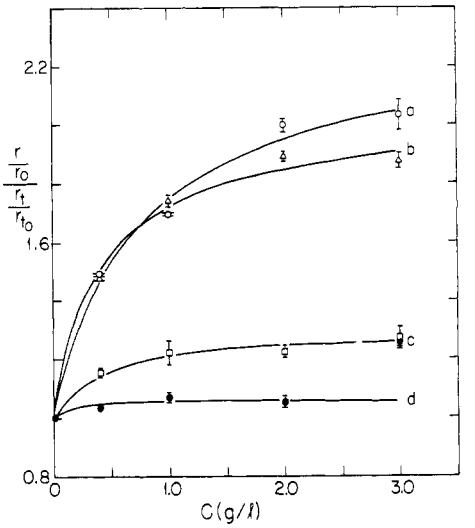

Figure 4. Dependence of the hydrodynamic radii of the spheres on the polymer concentration c, after correction for the non-Stokes–Einsteinian effects of Figure 3. Points are labeled as in Figure 1; the smooth curves are Langmuir adsorption isotherms.

Figure 3 shows the dependence of the hydrodynamic radius r_T (for spheres in the presence of Triton X-100) on polymer concentration, r_T being normalized by the radius r_{T0} of the same spheres in pure water–Triton X-100. The decrease in r_T/r_{T0} at higher polymer concentrations is due to non-Stokes–Einsteinian behavior, as discussed elsewhere.[1,2] The smooth curves in Figure 3 are fits to the form

$$r_T/t_{T0} = \exp(k_1 c^{k_2}) \qquad (2)$$

of Langevin and Rondelez;[4] values for k_1 and k_2 are in the caption.

Figure 3 may be said to give calibration data for the diffusion coefficient of Triton-coated particles of known sizes through different polymer solutions. These calibration curves are only weakly dependent on particle size; they

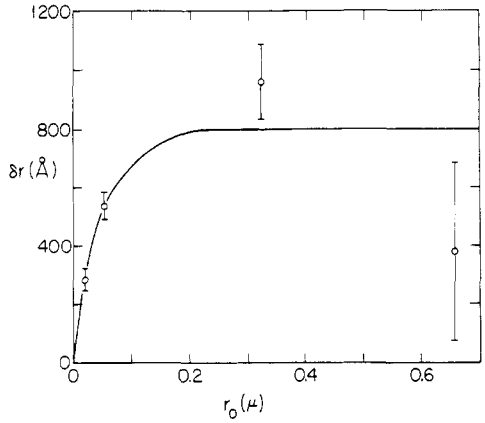

Figure 5. Dependence of the limiting thickness R of bound polymer at large c on the radius r_0 of the binding particle.

may therefore be used to correct the measured r of uncoated spheres for the failure of the Stokes–Einstein equation. A point-by-point comparison of Figures 1 and 3 leads to Figure 4, which shows only the changes in r due to polymer adsorption. Note in Figure 4 that, at high polymer concentration, r/r_0 rises to a constant value, rather than dropping off as in Figure 1.

The data in Figure 4 have the form of a Langmuir adsorption isotherm; adsorption parameters for each sphere size were calculated by fitting the data to[6]

$$c/(x/m) = c/a + 1/ab \qquad (3)$$

Here, c is the polymer concentration, a and b are parameters, and the amount of adsorbed polymer x/m was taken to be the change of volume of the spheres, as inferred from $r/(r_T/r_{T0})$. From a, the limiting thickness R of adsorbed polymer at large c can be calculated. For the smaller spheres, x/m does not attain values corresponding to R for any value of c below the solubility limit of the polymer. R values are in Figure 5.

From Figures 1 and 4, it is apparent that a considerable error would arise from use of the uncorrected values of r to calculate binding isotherms. In contrast to the corrected plots, the uncorrected plots of r/r_0 for the 0.322 and 0.655-μm spheres are not even equalitatively similar to Langmuir adsorption isotherms. To demonstrate that the combination of polymer adsorption and non-Stokes–Einsteinian effects give a reasonable reflection of the entirety of the data, rather than isolated portions of it, we show in Figure 1 (solid lines) the product of the adsorption isotherms (lines, Figure 4) and the fitted curves (eq 2) for the failure of the Stokes–Einstein equation.

Acknowledgment. We thank Professor P. J. Elving for this comments on an earlier draft of this paper. The support of this work by the National Science Foundation under Grant CHE82-13941 is gratefully acknowledged.

References and Notes

(1) Lin, T.-H.; Phillies, G. D. T. *J. Phys. Chem.* **1982**, *86*, 4073–4077.
(2) Lin, T.-H.; Phillies, G. D. J., in preparation.
(3) Tadros, T. F.; Vincent, B. *J. Phys. Chem.* **1980**, *84*, 1575–1580.
(4) Langevin, D.; Rondelez, F. *Polymer* **1978**, *19*, 875–882.
(5) Sperry, P. R. Abstracts of the 57th Colloid and Surface Science Symposium, Toronto, 1983.
(6) Adamson, A. "Physical Chemistry of Surfaces"; Wiley: New York, 1960.

Gregory Ullmann and George D. J. Phillies*
Department of Chemistry
The University of Michigan
Ann Arbor, Michigan 48109

Received July 19, 1983